Adaptive Output Feedback Control with Input Saturation

Bong-Jun Yang [1] , Anthony. J. Calise,[2] James I. Craig [3]
Georgia Institute of Technology
School of Aerospace Engineering
Atlanta, GA 30332

Abstract

We consider the problem of adaptive output feedback control in the presence of saturating input characteristic. The adaptive control architecture augments an existing linear control design. The approach is applicable to non-affine, nonlinear systems with both parametric uncertainty and unmodeled dynamics subject to input saturation. Boundedness of signals is shown through Lyapunov's direct method. Experimental results with a 3-disk torsional pendulum are presented to demonstrate the approach.

1 Introduction

Adaptive control can be used to robustify the design of a model based controller which is vulnerable to modelling error. Due to its *universal approximator* property [1], artificial neural networks (ANNs) have evolved as a powerful tool for designing an adaptive feedback controller for uncertain nonlinear systems [2–5].

In most cases, adaptive control design implies the replacement of the existing control system. If possible, it is highly desirable to augment an existing control system with an adaptive element. There have been attempts to augment an existing control system with an adaptive process [6–10]. A major limitation in these efforts is that they require state feedback. Moreover, most of these approaches require that the full dimension of the control system is known, therefore are not robust to unmodelled dynamics.

Recently, output feedback methods have been developed that do not require knowledge of the dimension of the plant [11,12]. These methods only require knowledge of the relative degree of the regulated output, and therefore are adaptive to unmodelled dynamics as well. The approaches in [13, 14] have extended the output feedback methodology of [11,12] from augmenting *inverting controllers* to augmenting *linear controllers*.

In assessing control system, one always encounters a fundamental problem that threatens the expected operation. All control actuation devices are subject to amplitude saturation. There have been many approaches which account for the capacity of the actuation device in relation to the control system performance in both adaptive and non-adaptive control designs [15–17]. Our work in this paper is mostly inspired by the approach called Pseudo Control Hedging(PCH) that, under actuator nonlinearities, permits correct adaptation of a NN in compensating for inexact inversion in a state feedback setting [17]. The main contribution of this paper is to prove the manner in which PCH should be incorporated so that adaptation is permitted in an output feedback setting in which the adaptive process augments a linear controller. We refer to this method as *control hedging*(CH), since its implementation involves actual control signals, and not pseudo controls. The method was first introduced in [14] without a stability proof.

The paper is organized as follows: After we formulate the control problem in Section 2, tracking error dynamics with CH are described in Section 3. The adaptive output feedback approach which augments the linear controller is summarized in Section 4, and its stability analysis is given in Section 5. Experimental results with a 3-disk torsional pendulum are presented to demonstrate the approach in Section 6. Finally, the paper is concluded in Section 7.

2 Problem Formulation

Let the *uncertain* system dynamics be given by:

$$\dot{\boldsymbol{x}}_p = \boldsymbol{f}_p(\boldsymbol{x}_p, u, \boldsymbol{d}), \quad y = h_p(\boldsymbol{x}_p, \boldsymbol{d}) \tag{1}$$

where $\boldsymbol{x}_p \in R^{n_p}$ are the states of the system, $u(t) \in R$ and $y(t) \in R$ are control and measurement variables, and $\boldsymbol{d}(t) \in R^{n_d}$ is the disturbance. We assume that the relative degree r of the system is known and that the system is globally exponentially minimum phase. The *bounded* disturbance $\boldsymbol{d}(t)$ evolves according to its own dynamics:

$$\dot{\boldsymbol{x}}_d = \boldsymbol{f}_d(\boldsymbol{x}_d), \quad \boldsymbol{d} = \boldsymbol{h}_d(\boldsymbol{x}_d) \tag{2}$$

where $\boldsymbol{x}_d(t) \in R^{n_d}$. The functions $\boldsymbol{f}_d$ and $\boldsymbol{h}_d$ are uncertain. The augmented system consisting of the plant and disturbance dynamics can now be expressed as:

$$\begin{aligned} \dot{\boldsymbol{x}} &= \boldsymbol{f}(\boldsymbol{x}, u), \; y = h(\boldsymbol{x}) \\ y^{(r)} &= h_r(\boldsymbol{x}, u) \end{aligned} \tag{3}$$

where $\boldsymbol{x}^T = [\, \boldsymbol{x}_p^T \; \boldsymbol{x}_d^T \,]$, $\boldsymbol{f}(\boldsymbol{x}, u) = \begin{bmatrix} \boldsymbol{f}_p(\boldsymbol{x}_p, u, \boldsymbol{h}_d(\boldsymbol{x}_d)) \\ \boldsymbol{f}_d(\boldsymbol{x}_d) \end{bmatrix}$, and $h(\boldsymbol{x}) = h_p(\boldsymbol{x}_p, \boldsymbol{h}_d(\boldsymbol{x}_d))$. We assume that the augmented system in (3) is *observable*. This can be almost always assured if the system in (1) is observable [13].

[1]Graduate Research Assistant, Student IEEE,AIAA member
[2]Professor, Member IEEE, Fellow AIAA
[3]Professor, Senior Member AIAA

0-7803-7896-2/03/$17.00

Proceedings of the American Control Conference
Denver, Colorado June 4-6, 2003

Let the plant model, which is used in control design, be described by:

$$\begin{aligned} \dot{\boldsymbol{x}}_m &= \boldsymbol{A}_m \boldsymbol{x}_m + \boldsymbol{B}_m u_{lc}, \; y_m = \boldsymbol{C}_m \boldsymbol{x}_m \\ y_m^{(r)} &= \hat{h}_r(\boldsymbol{x}_m, u_{lc}) = \boldsymbol{C}_r \boldsymbol{x}_m + D_r u_{lc} \end{aligned} \tag{4}$$

where $\boldsymbol{x}_m \in R^{m}$ $(m \leq n_p)$ and $\boldsymbol{C}_r = \boldsymbol{C}_m \boldsymbol{A}_m^r$, $D_r = \boldsymbol{C}_m \boldsymbol{A}_m^{r-1} \boldsymbol{B}_m$. The linear controller is defined by:

$$\begin{aligned} \dot{\boldsymbol{x}}_c &= \boldsymbol{A}_c \boldsymbol{x}_c + \boldsymbol{B}_c (y_c - y) \\ u_{lc} &= \boldsymbol{C}_c \boldsymbol{x}_c + D_c (y_c - y) \end{aligned} \tag{5}$$

The plant model in (4) regulated by the linear controller in (5), with the replacement y by y_m, results in the following nominal closed loop system:

$$\dot{\bar{\boldsymbol{x}}}^n = \boldsymbol{F} \bar{\boldsymbol{x}}^n + \boldsymbol{G}_c y_c(t), \; y^n = \boldsymbol{H} \bar{\boldsymbol{x}}^n \tag{6}$$

where $\bar{\boldsymbol{x}}^{n^T} = [\boldsymbol{x}_m^{n^T}, \; \boldsymbol{x}_c^{n^T}]^T$, and

$$\begin{aligned} \boldsymbol{F} &= \begin{bmatrix} \boldsymbol{A}_m - \boldsymbol{B}_m D_c \boldsymbol{C}_m & \boldsymbol{B}_m \boldsymbol{C}_c \\ -\boldsymbol{B}_c \boldsymbol{C}_m & \boldsymbol{A}_c \end{bmatrix} \\ \boldsymbol{G}_c &= \begin{bmatrix} \boldsymbol{B}_m D_c \\ \boldsymbol{B}_c \end{bmatrix}, \; \boldsymbol{H} = \begin{bmatrix} \boldsymbol{C}_m & 0 \end{bmatrix}, \end{aligned} \tag{7}$$

where $(\cdot)^n$ represents the nominal trajectory, and $y_c(t)$ is a bounded reference command. It is assumed that $y_c - y_m$ is bounded, and meets performance specifications by design. The control design process to augment an adaptive element, with a non-saturating input, is described in [13]. With the actuator saturation:

$$\delta = g(u) = \begin{cases} u, & \text{if } |u| \leq \delta_0 \\ \text{sgn}(u)\delta_0, & \text{if } |u| > \delta_0, \end{cases} \tag{8}$$

where u is the commanded control input and δ_0 is the control limit, the dynamics in (3) are written as:

$$\begin{aligned} \dot{\boldsymbol{x}} &= \boldsymbol{f}(\boldsymbol{x}, g(u)), \; y = h(\boldsymbol{x}) \\ y^{(r)} &= h_r(\boldsymbol{x}, g(u)) \end{aligned} \tag{9}$$

Our control objective is to augment u_{lc} in (5) with an adaptive signal u_{ad} so that bounded reference command tracking for the system in (9) can be achieved.

3 Output Tracking Error Equation

The PCH technique in [17] permits the adaptive process to continue to correct for modelling error under input saturation. The CH technique, PCH implementation in the context of augmenting a linear controller, is illustrated in Figure 1. Instead of pseudo control signals, the CH architecture involves control signals. The architecture without CH simply amounts to setting $u_h = 0$. If the output of the actuator δ in (8) is available, then $\hat{\delta} = \delta$ in Figure 1. Otherwise, we assume it is estimated using:

$$\hat{\delta} = \hat{g}(u) = \begin{cases} u, & \text{if } |u| \leq \hat{\delta}_0 \\ \text{sgn}(u)\hat{\delta}_0, & \text{if } |u| > \hat{\delta}_0, \end{cases} \tag{10}$$

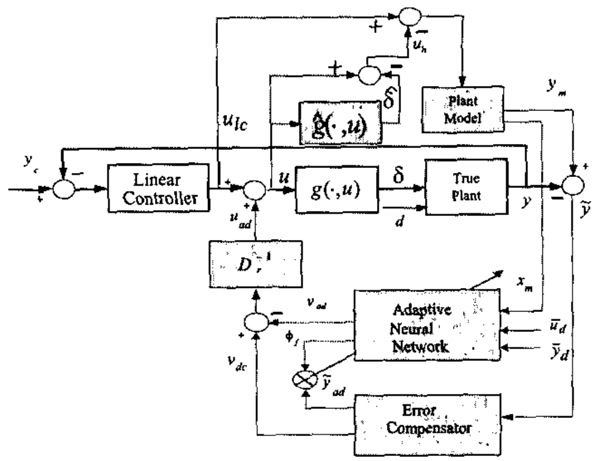

Figure 1: Controller Architecture with Control Hedging.

where $\hat{\delta}_0$ is an estimate for δ_0. With CH, the plant model dynamics in (4) are modified as follows:

$$\begin{aligned} \dot{\boldsymbol{x}}_m &= \boldsymbol{A}_m \boldsymbol{x}_m + \boldsymbol{B}_m (u_{lc} - u_h), \\ y_m^{(r)} &= \boldsymbol{C}_r \boldsymbol{x}_m + D_r (u_{lc} - u_h), \end{aligned} \tag{11}$$

where $u_h = u - \hat{\delta}$, and can be expressed explicitly as:

$$u_h = \begin{cases} 0 & \text{if } |u| \leq \hat{\delta}_0 \\ u_{h_2} = u - \text{sgn}(u)\hat{\delta}_0 & \text{if } |u| > \hat{\delta}_0 \end{cases} \tag{12}$$

Let the output tracking error $\tilde{y} \triangleq y_m - y$, then the plant model dynamics in (11) regulated by the linear controller in (5) can be described by :

$$\dot{\bar{\boldsymbol{x}}} = \boldsymbol{F} \bar{\boldsymbol{x}} + \boldsymbol{G}_c y_c + \boldsymbol{G}_c \tilde{y} - \boldsymbol{G} u_h, \tag{13}$$

where $\bar{\boldsymbol{x}}^T = [\boldsymbol{x}_m^T, \; \boldsymbol{x}_c^T]^T$, $\boldsymbol{G}^T = [\boldsymbol{B}_m^T, \; 0^T]^T$. Define the plant model error vector: $\boldsymbol{e}_m \triangleq \bar{\boldsymbol{x}}^n - \bar{\boldsymbol{x}}$, then comparing (13) to (6) leads to the following *plant model error dynamics*:

$$\dot{\boldsymbol{e}}_m = \boldsymbol{F} \boldsymbol{e}_m - \boldsymbol{G}_c \tilde{y} + \boldsymbol{G} u_h. \tag{14}$$

Since $\boldsymbol{F}$ is Hurwitz by design, for any $Q_n > 0$, there exists $P_n > 0$ such that:

$$\boldsymbol{F}^T P_n + P_n \boldsymbol{F} + Q_n = 0. \tag{15}$$

With $\hat{h}_r$ in (4) and $\hat{\delta}$ in (10), $y^{(r)}$ in (9) can be written as:

$$y^{(r)} = \boldsymbol{C}_r \boldsymbol{x}_m + D_r \hat{\delta} + \Delta(\boldsymbol{x}, \boldsymbol{x}_m, u), \tag{16}$$

$$\Delta(\boldsymbol{x}, \boldsymbol{x}_m, u) = h_r(\boldsymbol{x}, \delta) - \hat{h}_r(\boldsymbol{x}_m, \hat{\delta}) \tag{17}$$

Let $u = u_{lc} + u_{ad}$, then comparing (11) and (16) leads to the following *output tracking error dynamics*:

$$\tilde{y}^{(r)} = -D_r u_{ad} - \Delta(\boldsymbol{x}, \boldsymbol{x}_m, u). \tag{18}$$

With the definition: $u_{ad} = D_r^{-1}(\nu_{dc} - \nu_{ad})$, the output tracking error dynamics in (18) is finally written as:

$$\tilde{y}^{(r)} = -\nu_{dc} + \nu_{ad} - \Delta \tag{19}$$

where ν_{dc} is the output of a linear controller, with $\tilde{y}$ as its input, that is designed to stabilize the error dynamics when $\Delta(\boldsymbol{x}, \boldsymbol{x}_m, u) = 0$, and ν_{ad} is the output of a NN, whose weights are adapted in a way to guarantee a bounded error response. The form of error dynamics in (19) is the same as one would obtain if $\delta = u$ (no input saturation), with the exception that both δ and $\hat{\delta}$ in (17) are replaced by u. From (19), it follows that Δ depends on ν_{ad} through u, whereas ν_{ad} is designed to cancel Δ. The following assumption is imposed to guarantee the existence and uniqueness of a solution for ν_{ad}.

Assumption 1 *The mapping $\nu_{ad} \mapsto \Delta$ is a contraction.*

Remark 1: It has been shown in [11] that, in the absence of saturation, Assumption 1 is equivalent to the following two conditions:

$$\text{sign}(D_r) = \text{sign}(\frac{\partial h_r}{\partial u}), \ \frac{|\frac{\partial h_r}{\partial u}|}{2} < |D_r| < \infty. \qquad (20)$$

These conditions imply that control reversal is not permitted, and impose a lower bound on the estimate of the control effectiveness D_r of the plant model. When both the true and the estimated control positions are at their limits, Δ is independent of ν_{ad} and there is no fixed point issue. When the true control is at its limit, but its estimate is not (or when CH is not used at all), $\nu_{ad} - \Delta$ is independent of ν_{ad}, and there is no solution. On the other hand, during periods of time when the estimated control position is on its limit, but the true control position is not, then (20) reduces to:

$$\left|\frac{\partial \Delta}{\partial \nu_{ad}}\right| = \left|\frac{\partial h_r}{\partial u} D_r^{-1}\right| < 1 \Longleftrightarrow |D_r| > \left|\frac{\partial h_r}{\partial u}\right|. \qquad (21)$$

Knowledge of the sign of the control effectiveness is still required to stabilize the system in Section 4. In summary, it is desirable to underestimate the control limit, and overestimate the control effectiveness.

4 Adaptive Output Feedback Augmentation

The approach in [11] allows for designing the signals ν_{dc} and ν_{ad} in (19) using only available measurements. The error compensator has two outputs:

$$\begin{bmatrix} \nu_{dc}(s) \\ \tilde{y}_{ad}(s) \end{bmatrix} = \frac{1}{D_{dc}(s)} \begin{bmatrix} N_{dc}(s) \\ N_{ad}(s) \end{bmatrix} \tilde{y}(s). \qquad (22)$$

We assume that $D_{dc}(s)$ is a Hurwitz polynomial. With the error compensator in (22), the error equation given in (19) results in the following transfer function from $\nu_{ad} - \Delta$ to $\tilde{y}_{ad}$.

$$\begin{aligned} \tilde{y}_{ad}(s) &= \frac{N_{ad}(s)}{s^r D_{dc}(s) + N_{dc}(s)} (\nu_{ad} - \Delta) \\ &\equiv G(s)(\nu_{ad} - \Delta). \end{aligned} \qquad (23)$$

A linearly parameterized NN is used to approximate Δ defined in (17). Given $\epsilon > 0$, Δ can be approximated by a linearly parameterized NN over a compact domain with bounded weights $\boldsymbol{W}$ and a suitable set of basis functions $\phi(\cdot)$ that provide a universal approximation [11]:

$$\Delta = \boldsymbol{W}^T \phi(\boldsymbol{\eta}) + \varepsilon(\boldsymbol{\eta}), \ \|\varepsilon(\boldsymbol{\eta})\| < \epsilon, \qquad (24)$$

where $\varepsilon(\boldsymbol{\eta})$ is NN reconstruction error, and $\boldsymbol{\eta}$ is the network input vector:

$$\begin{aligned} \boldsymbol{\eta}(t) &= \begin{bmatrix} 1 & \boldsymbol{x}_m(t)^T & \bar{u}_d^T(t) & \bar{y}_d^T(t) \end{bmatrix}^T, \\ \bar{u}_d^T(t) &= [u(t) \quad u(t-d) \quad \cdots u(t-(n_1-r-1)d)]^T, \\ \bar{y}_d^T(t) &= [y(t) \quad y(t-d) \cdots y(t-(n_1-1)d)]^T, \end{aligned} \qquad (25)$$

where $n_1 \geq n$ is the length of a sliding window of measurements, r is the relative degree, and $d > 0$ is a positive time delay. The output of the adaptive NN in Figure 1 is designed as:

$$\nu_{ad} = \hat{\boldsymbol{W}}^T \phi(\boldsymbol{\eta}) \qquad (26)$$

where $\hat{\boldsymbol{W}}$ are estimates of the weights $\boldsymbol{W}$ in (24) that are adjustable on-line. For the NN adaptation rule to be realizable, $G(s)$ in (23) is required to be strictly positive real (SPR) [11]. For that purpose, a stable low pass filter $T^{-1}(s)$ is introduced so that $G(s)T(s)$ is SPR in case $r > 1$.

$$\tilde{y}_{ad}(s) = G(s)T(s)[T^{-1}(s)(\nu_{ad} - \Delta)], \qquad (27)$$

where the polynomial $T(s)$ is Hurwitz, but can otherwise be freely chosen. For convenience in analysis, it is assumed that the filter $T^{-1}(s)$ is scaled so that its maximum gain is unity. The filter is realized by:

$$\dot{\boldsymbol{z}}_f = \boldsymbol{A}_f \boldsymbol{z}_f + \boldsymbol{B}_f \phi, \ \phi_f = \boldsymbol{C}_f \boldsymbol{z}_f. \qquad (28)$$

Since A_f is Hurwitz, for any $Q_f > 0$ there exist $P_f > 0$ such that:

$$\boldsymbol{A}_f^T P_f + P_f \boldsymbol{A}_f + Q_f = 0. \qquad (29)$$

Figure 2 depicts the flow of signals involved in design of ν_{dc} and the SPR filter $T(s)$. The filtered NN

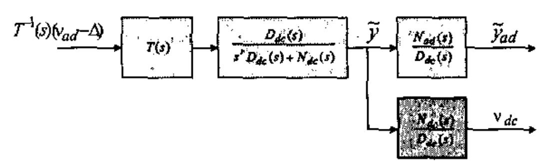

Figure 2: Block Diagram for Output Tracking Error Dynamics

reconstruction error, $\psi \triangleq T^{-1}(s)(\nu_{ad} - \Delta)$, can be written as: $\psi = \tilde{\boldsymbol{W}}^T \phi_f + \theta - \varepsilon_f$ and ε_f are the signals ϕ and ε, respectively, after being filtered through $T^{-1}(s)$, and θ is the mismatch term given by $\theta(s) = T^{-1}(s)(\tilde{\boldsymbol{W}}^T \phi) - \tilde{\boldsymbol{W}}^T \phi_f$. The terms $\theta(s)$ and ε_f can be bounded as:

$$\|\theta\| \leq \alpha \left\|\tilde{\boldsymbol{W}}\right\|_F, \ \alpha > 0, \quad |\varepsilon_f| \leq \epsilon, \qquad (30)$$

Proceedings of the American Control Conference
Denver, Colorado June 4-6, 2003

where $\tilde{\boldsymbol{W}} = \hat{\boldsymbol{W}} - \boldsymbol{W}$ represents weight deviations from ideal weights $\boldsymbol{W}$. The transfer function from ψ to $\tilde{y}$ is realized as follows (see Figure 2):

$$\dot{\boldsymbol{z}}_e = \boldsymbol{A}_e \boldsymbol{z}_e + \boldsymbol{B}_e \psi, \; \tilde{y} = \boldsymbol{C}_e \boldsymbol{z}_e \tag{31}$$

The transfer functions from $\tilde{y}$ to $\tilde{y}_{ad}$ and ν_{dc}, are realized as follows:

$$\begin{aligned} \dot{\boldsymbol{z}}_{dc} &= \boldsymbol{A}_{dc}\boldsymbol{z}_{dc} + \boldsymbol{B}_{dc}\tilde{y}, \; \tilde{y}_{ad} = \boldsymbol{C}_{ad}\boldsymbol{z}_{dc} + D_{ad}\tilde{y} \\ \nu_{dc} &= \boldsymbol{C}_{dc}\boldsymbol{z}_{dc} + D_{dc}\tilde{y} \end{aligned} \tag{32}$$

With the definition $\boldsymbol{z}^T = [\boldsymbol{z}_e^T, \; \boldsymbol{z}_{dc}^T]^T$, combining (31) and (32) leads to the following *non-minimal* realization for the tracking error dynamics in Figure 2.

$$\begin{aligned} \dot{\boldsymbol{z}} &= \boldsymbol{A}_{cl}\boldsymbol{z} + \boldsymbol{B}_{cl}\psi \\ \tilde{y}_{ad} &= \boldsymbol{C}_{cl}\boldsymbol{z}, \; \nu_{dc} = \boldsymbol{C}_{\nu}\boldsymbol{z}, \; \tilde{y} = \boldsymbol{C}_{\tilde{y}}\boldsymbol{z} \end{aligned} \tag{33}$$

where $\boldsymbol{A}_{cl} = \begin{bmatrix} \boldsymbol{A}_e & \boldsymbol{0} \\ \boldsymbol{B}_{dc}\boldsymbol{C}_e & \boldsymbol{A}_{dc} \end{bmatrix}$, $\boldsymbol{B}_{cl} = \begin{bmatrix} \boldsymbol{B}_e \\ 0 \end{bmatrix}$, $\boldsymbol{C}_{cl} = \begin{bmatrix} D_{ad}\boldsymbol{C}_e & \boldsymbol{C}_{ad} \end{bmatrix}$, $\boldsymbol{C}_{\nu} = \begin{bmatrix} D_{dc}\boldsymbol{C}_e & \boldsymbol{C}_{dc} \end{bmatrix}$, $\boldsymbol{C}_{\tilde{y}} = \begin{bmatrix} \boldsymbol{C}_e & \boldsymbol{0} \end{bmatrix}$. Since the transfer function from ψ to $\tilde{y}_{ad}$ is SPR, by the Meyer-Kalman-Yakubovitz(MKY) Lemma [18], there exist $Q > 0$ and $P > 0$ such that:

$$\boldsymbol{A}_{cl}^T P + P\boldsymbol{A}_{cl} + Q = 0, \; P\boldsymbol{B}_{cl} = \boldsymbol{C}_{cl}^T. \tag{34}$$

The signals ϕ_f are used in the following NN adaptation rule:

$$\dot{\hat{\boldsymbol{W}}} = -\Gamma_W[\tilde{y}_{ad}\boldsymbol{\phi}_f + \sigma\hat{\boldsymbol{W}}] \tag{35}$$

where $\Gamma_W > 0$ is the adaptation gain, defining the "learning rate" and $\sigma\hat{W}$ is the $\sigma-$modification term [4].

5 Stability Analysis

With Eq.s (5), (26), (32), the control hedging signal u_{h_2} in (12) can be written as follows:

$$u_{h_2} = u_{h_2}^* - D_r^{-1}\tilde{\boldsymbol{W}}^T\boldsymbol{\phi}(\boldsymbol{\eta}) \tag{36}$$

where $u_{h_2}^* = J_1\boldsymbol{e}_m + J_2\boldsymbol{z} + D_c y_c - D_r^{-1}\boldsymbol{W}^T\boldsymbol{\phi}(\boldsymbol{\eta}) - \text{sign}(u)\hat{\delta}_0$, $J_1 = [-D_c\boldsymbol{C}_m, \; \boldsymbol{C}_c]$, and $J_2 = \left((D_c - D_r^{-1}D_{dc})\boldsymbol{C}_{\tilde{y}} - D_r^{-1}[\,0, \; \boldsymbol{C}_{dc}]\right)$. It is assumed that u_{h_2} satisfies a linear growth condition in the domain of interest.

Assumption 2 $|u_{h_2}| \le \mu_1 \|e_m\| + \mu_2 \|z\| + \mu_3 \left\|\tilde{\boldsymbol{W}}\right\| + \mu_4$, for $e_m \in \Omega_{\boldsymbol{e}_m}$, $\boldsymbol{z} \in \Omega_{\boldsymbol{z}}$

We will show via Lyapunov's direct method that the signals $\boldsymbol{e}_m$ in (14), $\boldsymbol{z}$ in (33), $\boldsymbol{z}_f$ in (28), and the NN weight errors $\tilde{\boldsymbol{W}}$, are bounded. With that objective in mind, we define the error vector space $\zeta^T \triangleq [\,\boldsymbol{e}_m^T \, \boldsymbol{z}^T \, \boldsymbol{z}_f^T \, \tilde{\boldsymbol{W}}^T\,]$ which belongs to the convex compact set $\mathcal{B}_R \triangleq \{\zeta | \, \|\zeta\| \le R, \; R > 0\} \subseteq \Omega_{\boldsymbol{e}_m} \times \Omega_{\boldsymbol{z}} \times \Omega_{\boldsymbol{z}_f} \times \Omega_{\tilde{\boldsymbol{W}}}$ such that for every $\zeta \in \mathcal{B}_R$, the NN approximation implied in (24) is valid. Consider the following Lyapunov function:

$$\begin{aligned} L(\zeta) = \zeta^T T \zeta &= \frac{1}{2}\boldsymbol{e}_m^T P_n \boldsymbol{e}_m + \frac{1}{2}\boldsymbol{z}^T P \boldsymbol{z} \\ &+ \frac{1}{2}\boldsymbol{z}_f P_f \boldsymbol{z}_f + \frac{1}{2} tr\{\tilde{\boldsymbol{W}}^T \Gamma_W^{-1} \tilde{\boldsymbol{W}}\} \end{aligned} \tag{37}$$

where $P_n, P, P_f > 0$ are solutions of (15), (34), (29) respectively and T is defined to be:

$$T = \frac{1}{2}\begin{bmatrix} P_n & 0 & 0 & 0 \\ 0 & P & 0 & 0 \\ 0 & 0 & P_f & 0 \\ 0 & 0 & 0 & \Gamma_W^{-1} \end{bmatrix} \tag{38}$$

Introduce T_m, T_M which are minimal and maximal eigenvalues of T respectively. Then $T_m \|\zeta\|^2 \le L(\zeta) \le T_M \|\zeta\|^2$. Let $\alpha = \sqrt{\frac{T_m}{T_M}}R, \mathcal{B}_\alpha = \{\zeta \in \mathcal{B}_R | \, \|\zeta\| \le \alpha\}$.

Theorem 1 *Suppose $\zeta(0) \in \mathcal{B}_\alpha$ and $R > C$, which is defined later in (42). Subject to assumptions 1-2, the control design described in Figure 1 guarantees that the signal ζ is uniformly ultimately bounded(UUB) with the bound $\sqrt{\frac{T_M}{T_m}}C$, provided the following conditions hold:*

$$\begin{aligned} \gamma_1 &> \gamma_4 \\ \lambda_{\min}(Q) &> 2\epsilon \|P\boldsymbol{B}_{cl}\| + \frac{4\gamma_2^2}{\gamma_1} \\ \lambda_{\min}(Q_f) &> \|P_f \boldsymbol{B}_f\| \, \|\phi\| \\ \sigma &> 1 + \frac{\gamma_3^2}{\gamma_1} + \frac{\alpha^2 \|P\boldsymbol{B}_{cl}\|^2}{\lambda_{\min}(Q)} \end{aligned} \tag{39}$$

where $\gamma_1 = \frac{1}{2}\lambda_{\min}(P_n) - \mu_1 \|P_n\boldsymbol{G}\|$, $\gamma_2 = \|P_n\boldsymbol{G}_c\boldsymbol{C}_{\tilde{y}}\| + \mu_2 \|P_n\boldsymbol{G}\|$, $\gamma_3 = \mu_3 \|P_n\boldsymbol{G}\|$, $\gamma_4 = \mu_4 \|P_n\boldsymbol{G}\|$.

Proof: Consider the Lyapunov function L in (37). Using the fact that:$\boldsymbol{z}^T P\boldsymbol{B}_{cl} = \boldsymbol{z}^T\boldsymbol{C}_{cl}^T = \tilde{y}_{ad}$ by (34), together with the dynamics described in (14), (33) and (28), applying the NN weights update rule given in (35) leads to the following time derivative of L:

$$\begin{aligned} \dot{L} =& \boldsymbol{e}_m^T P_n[\boldsymbol{F}\boldsymbol{e}_m - \boldsymbol{G}_c\tilde{y} + \boldsymbol{G}u_h] - \frac{1}{2}\boldsymbol{z}^T Q\boldsymbol{z} \\ &+ \boldsymbol{z}^T P\boldsymbol{B}_{cl}(\theta - \varepsilon_f) - \frac{1}{2}\boldsymbol{z}_f^T Q_f \boldsymbol{z}_f \\ &+ \boldsymbol{z}_f^T P_f \boldsymbol{B}_f \phi - \sigma tr\{\tilde{\boldsymbol{W}}^T(\tilde{\boldsymbol{W}} + \boldsymbol{W})\} \end{aligned} \tag{40}$$

We show that depending on whether the estimated control $\hat{\delta}$ is in saturation or not, the time derivative of Lyapunov function $\dot{L}$ is negative outside different compact sets.

i) when $u_h = u_{h_2}$, following lines similar to the proofs in [11,12], it can be shown that:

$$\dot{L} \le -\kappa_{\boldsymbol{e}_m}\|e_m\|^2 - \kappa_{\boldsymbol{z}}\|\boldsymbol{z}\|^2 - \kappa_{\boldsymbol{z}_f}\|\boldsymbol{z}_f\|^2 - \kappa_W\left\|\tilde{\boldsymbol{W}}\right\|_F^2 + \Upsilon^2 \tag{41}$$

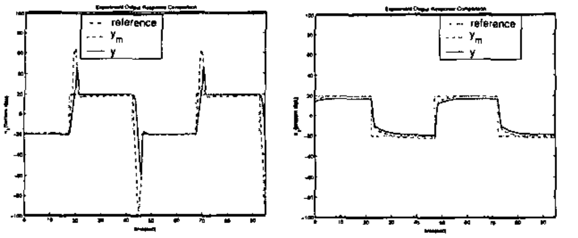

(a) without CH (b) with CH

Figure 3: Responses of Plant Model,y_m, and the output, y with no external disturbance

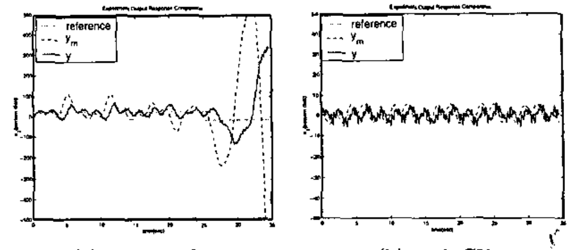

(a) without CH (b) with CH

Figure 4: Responses of Plant Model,y_m, and the output, y with big external disturbance

where $\kappa_{e_m} = \frac{1}{2}(\gamma_1 - \gamma_4)$, $\kappa_z = \frac{1}{4}\lambda_{\min}(Q) - \frac{\beta_2}{2} - \frac{\gamma_2^2}{\gamma_1}$, $\kappa_{z_f} = \frac{1}{2}(\lambda_{\min}(Q_f) - \beta_3)$, $\kappa_W = \sigma - 1 - \frac{\gamma_3^2}{\gamma_1} - \frac{\beta_1^2}{\lambda_{min}(Q)}$, $\Upsilon^2 = \frac{1}{2}[\gamma_4 + \beta_2 + \beta_3 + \frac{\sigma^2 W^{*2}}{2}]$, $\beta_1 = \alpha\|PB_{cl}\|$, $\beta_2 = \epsilon\|PB_{cl}\|, \beta_3 = \|P_f B_f \phi\|$. Define a compact set $\mathcal{B}_C = \{\zeta \in \mathcal{B}_R \mid \|\zeta\| \le C\}$, where

$$C = \max\left\{\sqrt{\frac{\Upsilon^2}{\kappa_{e_m}}}, \sqrt{\frac{\Upsilon^2}{\kappa_z}}, \sqrt{\frac{\Upsilon^2}{\kappa_{z_f}}}, \sqrt{\frac{\Upsilon^2}{\kappa_W}}\right\}. \tag{42}$$

Then $\dot{L} < 0$ when $\|\zeta\| > C$. Define $\rho = \sqrt{\frac{T_M}{T_m}}C$, $\mathcal{B}_\rho = \{\zeta \in \mathcal{B}_R | \|\zeta\| \le \rho\}$, then ζ is UUB in $\mathcal{B}_\rho$ [19, Corollary 5.1].

ii) when $u_h = 0$, it can be shown in the same manner as when $u_h = u_{h_2}$ that $\dot{L} < 0$ outside the ball $\mathcal{B}_{C_2} \subset \mathcal{B}_C$. The constant $C_2 < C$ can be found by setting $\mu_1 = \mu_2 = \mu_3 = \mu_4 = 0$ in (42). Thus ζ is UUB in $\mathcal{B}_\rho$.

From **i)** and **ii)**, it follows that $\zeta(t)$ is UUB in $\mathcal{B}_\rho$ regardless whether $\hat{\delta}$ saturates or not. □

The UUBness of e_m and z guarantees that the tracking error is bounded, since $|y_c - y| \le |y_c - y^n| + |y^n - y_m| + |\tilde{y}| \le |y_c - y^n| + \|C_m\|\,\|e_m\| + \|C_{\tilde{y}}\|\,\|z\|$, where $|y_c - y^n|$ represents the bound for tracking error of the nominal closed loop in (6).

Remark 2: According to Eq.(36), whether the control is in continual saturation depends on the nominal closed loop performance(through $\bar{x}^n$, y_c), the modelling error (through $W^T\phi(\eta)$), and the degree of NN adaptation to the modelling error (through e_m, z, $\tilde{y}$). Depending on specific control applications and available control authority, many variations may occur in their combinations. For example, if the modelling error gradually decreases as $y \to y_m$, the NN adapts well to the modelling error, the control system is subject to small external disturbances, and y_c is applied such that it can be tracked with a bounded control, then the control moves out of saturation after an initial saturation transient. In this case, if we define:$\rho_2 = \sqrt{\frac{T_M}{T_m}}C_2 < \rho$, $\mathcal{B}_{\rho_2} = \{\zeta \in \mathcal{B}_R | \|\zeta\| \le \rho_2\}$, then ζ is UUB in $\mathcal{B}_{\rho_2}$, i.e., a smaller bound is achieved(see Figure 3). On the other hand, if the modelling error is too large to be cancelled with bounded control, then the control will be in continual saturation and ζ is UUB in $\mathcal{B}_\rho$(see Figure 4).

Remark 3: The assumption that $\zeta(0) \in \mathcal{B}_\alpha$ requires that the control system initially belongs to the domain where stabilization is possible, because when $\zeta \in \mathcal{B}_\alpha \setminus \mathcal{B}_C$, $\dot{L} < 0$. If the system initially belongs to the region in which it cannot be stabilized, the control hedging signal u_h goes unbounded, resulting in $e_m \notin \Omega_{e_m}$ after some time.

Remark 4: The closed loop system when NN adaptation is complete, i.e., $\tilde{W} = 0$, is defined as a *non-adaptive subsystem* in [20]. The performance of this system represents the best performance that can be achieved with the CH together with the NN based adaptive element. The UUB region, in this case, further shrinks, because all the constants related to $\tilde{W}$ vanishes from C in (42).

6 Experimental Results with a 3-disk Torsional Pendulum System

The CH technique is tested in a 3-disk torsional pendulum system depicted in Figure 5. (Details of the system characteristics and control design are given in [14].) The control input u is the applied voltage, and the regulated output y variable is the angular displacement of the bottom disk. The transfer function is given by the 6th order model derived by experimental system identification:

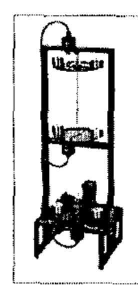

Figure 5: The 3-disk Torsional Pendulum System [21].

$$\frac{y}{u} = \frac{K_a(s^2 + 2\zeta_{z_1}\omega_{z_1}s + \omega_{z_1}^2)(s^2 + 2\zeta_{z_2}\omega_{z_2}s + \omega_{z_2}^2)}{s(s+c)(s^2 + 2\zeta_{p_1}\omega_{p_1}s + \omega_{p_1}^2)(s^2 + 2\zeta_{p_2}\omega_{p_2}s + \omega_{p_2}^2)} \tag{43}$$

Proceedings of the American Control Conference
Denver, Colorado June 4-6, 2003

The parameters are: $K_a = 40.46$, $\zeta_{z_1} = 0.009$, $\omega_{z_1} = 9.87$, $\zeta_{z_2} = 0.0035$, $\omega_{z_2} = 25.8$, $c = 0.1786$, $\zeta_{p_1} = 0.00559$, $\omega_{p_1} = 16(rad/sec)$ and $\zeta_{p_2} = 0.00323$, $\omega_{p_2} = 27.7(rad/sec)$. The plant model is, with flexibilities of shafts being unmodelled, given by:

$$\frac{y}{u} = \frac{K}{s(s+c)} \tag{44}$$

where $K = 13.49, c = 0.18$. The linear controller is designed as a lead compensator, which results in a dominant mode at $\omega_n = 3rad/s$ and $\zeta = 0.8$ for the nominal system design. This resulted in:

$$u_{lc} = K_1 \frac{s+b_1}{s+a_1}(y_c - y) \tag{45}$$

where $K_1 = 0.67, a_1 = 4.8, b_1 = 0.1786$.

In the first experiment, the control voltage is limited to 0.18 V. Fig. 3 compares the output tracking performances when the reference command is a square wave. The response without CH exhibits a large overshoot, which is similar to the effect of integrator windup in a non-adaptive system. With CH, the control system moves quickly out of initial phase saturation and gradually tracks the reference command without control saturation.

In the next experiment, a non-collocated disturbance is applied as an external torque to the top disk. The control voltage limit, 0.3 V, is intentionally set to demonstrate the CH technique when the control voltage is insufficient to cancel the applied disturbance. The reference command is set to zero, and the disturbance is constructed as $V_d(t) = 0.5(\sin t + \sin 3t + \sin 12t + \sin 15.7t + \sin 27.7t)$. Fig. 4(a) shows that without CH, the response exhibits an instability. The NN weights exhibit the same instability. With CH, Fig. 4(b) shows that while the disturbance is not completely rejected, the output $y(t)$ tracks the plant model $(y_m(t))$. This implies that correct adaptation is being achieved under continual control saturation.

7 Summary

This paper provides detailed analysis of, and theoretical justification for the CH technique introduced in [14]. Experimental results obtained using a 3-disk torsional pendulum laboratory model illustrate the effectiveness of the CH technique in permitting adaptation during periods of control saturation.

References

[1] N. Hornik, M. Stinchcombe, and H. White. Multilayer feedforward networks are universal approximators. *Neural Networks*, 2:359–366, 1989.

[2] K.S. Narendra. Neural networks for control: Theory and practice. *Proceedings of the IEEE*, 84(10):1385–1996, Oct. 1996.

[3] M.M. Polycarpou. Stable adaptive neural control scheme for nonlinear systems. *IEEE Transactions on Automatic Control*, 41(3):447–451, 1996.

[4] F.L. Lewis, S. Jagannathan, and A. Yeşildirek. *Neural Network Control of Robot Manipulators and Nonlinear Systems.* Taylor & Francis, 1999.

[5] S.S. Ge, C.C. Hang, T.H. Lee, and T. Zhang. *Stable Adaptive Neural Network Control.* Kluwer Academic Publishers, 2002.

[6] S. Ananthakrishnan. Adaptive tachometer feedback augmentation of the shuttle remote manipulator control system. In *IEEE International Conference on Robotics and Automation*, 1995.

[7] M.B. McFarland and D.T. Stansbury. Adaptive nonlinear autopilot for air-to-air missiles. In *AIAA Missiles Sciences Conference*, CA, 1998.

[8] G.A. Rovithakis. Robustifying nonlinear systems using high-order neural network controller. *IEEE Transactions on Automatic Control*, 44:102–108, 1999.

[9] M. Sharma and A.J. Calise. Neural network augmentation of existing linear controllers. In *Proceedings of the AIAA Guidance, Navigation, and Control Conference*, Montreal, Canada, August 2001.

[10] Y. Li, N. Sundararajan, and P. Saratchandran. Neuro-controller design for nonlinear fighter aircraft maneuver using fully tuned RBF networks. *Automatica*, 37:1293–1301, 2001.

[11] A.J. Calise, N. Hovakimyan, and M. Idan. Adaptive output feedback control of nonlinear systems using neural networks. *Automatica*, 37:1201–1211, 2001.

[12] N. Hovakimyan, F. Nardi, N. Kim, and A.J. Calise. Adaptive output feedback control of uncertain systems using single hidden layer neural networks. *IEEE Transactions on Neural Networks*, 13(6), 2002.

[13] A.J. Calise, B.-J. Yang, and J.I. Craig. Augmentation of an existing linear controller with an adaptive element. In *Proceedings of the American Control Conference*, pages 1549–1554, Anchorage,AK, May 2002.

[14] A.J. Calise, B.-J. Yang, and J.I. Craig. An augmenting adaptive approach to control of flexible systems. In *Proceedings of AIAA guidance,navigation and control conference*, 2002.

[15] Ali Saberi, Anton A. Stoorvogel, and Peddapullaiah Sannuti. *Control Of Linear Systems with Regulation and Input Constraints.* Springer-Verlag, 2000.

[16] S.P. Karason and A.M. Annaswamy. Adaptive control in the presence of input constraints. *IEEE Transactions on Automatic Control*, 39(11):1–6, 1994.

[17] Eric N. Johnson and Anthony J. Calise. Neural network adaptive control of systems with input saturation. In *Proceedings of the American Control Conference*, Arlington, Virginia, jun 2001.

[18] P.A. Ioannou and J. Sun. *Robust Adaptive Control.* Prentice-Hall, Englewood Cliffs, NJ, 1996.

[19] H.K. Khalil. *Nonlinear Systems.* Prentice-Hall, 1996.

[20] Eric Norman Johnson. *Limited Authority Adaptive Flight Control.* PhD thesis, Georgia Institute of Technology, School of Aerospace Engineering, December 2000.

[21] Torsion pendulum appratus, ECP Systems, Inc. `http://www.ecpsystems.com/controls/torplant.htm`.